Chinese Chemical Letters 37 (2026) 111535

Contents lists available at ScienceDirect

Chinese Chemical Letters

journal homepage: www.elsevier.com/locate/cclet

Particleization of cyclic trinuclear complexes into hybrid nanoparticles using diblock copolymers

Huahua Cui, Baiyao Liu, Qin Li, Guo-Quan Huang, Xu Chen, Biao Xiong, Jiahao Zhang, Ji Zheng*, Rong-Jia Wei*, Yin Ning*, Dan Li

College of Chemistry and Materials Science, Guangdong Provincial Key Laboratory of Supramolecular Coordination Chemistry, Jinan University, Guangzhou 510632, China

ARTICLE INFO

Article history:
Received 5 March 2025
Revised 30 June 2025
Accepted 2 July 2025
Available online 3 July 2025

Keywords:
Hybrid nanoparticles
Diblock copolymers
Cyclic trinuclear complexes
Sonogashira cross-coupling reaction
Colloidal stability

ABSTRACT

Cyclic trinuclear complexes (CTCs) are coordination compounds composed of three metal atoms arranged in a cyclic structure, which imparts them with significant potential for catalytic applications. However, their practical use is often hindered by issues of low chemical stability and poor dispersity. In this work, we present an efficient strategy for stabilizing trinuclear copper complexes [tris(μ_2–4-carboxaldehyde-pyrazolato-*N,N'*)-tri-copper(I) monohydrate, $Cu_3(PyCA)_3{\cdot}H_2O$] by chemically incorporating them into the core of diblock copolymer aggregates. Specifically, we utilize reversible addition-fragmentation chain transfer (RAFT) polymerization to synthesize poly(2-aminoethyl methacrylate hydrochloride)$_{50}$-*block*-poly(glycerol monomethacrylate)$_{52}$ (A_{50}-G_{52}) diblock copolymers. The subsequent reaction between primary amine groups of the A_{50} block and aldehyde groups of the $Cu_3(PyCA)_3{\cdot}H_2O$ leads to the formation of A_{50}-G_{52}-$Cu_3(PyCA)_3$ hybrid nanoparticles, in which the G_{52} blocks serve as steric coronas, while the $Cu_3(PyCA)_3{\cdot}H_2O$ are incorporated within the core domain. Notably, these hybrid nanoparticles exhibit enhanced stability and improved catalytic performance in the Sonogashira cross-coupling reaction in air. Through the precise design of reactive block copolymers, this study presents a novel strategy for the particleization of CTCs, thereby enabling the practical and scalable preparation of a diverse range of CTCs-based functional materials with enhanced properties.

© 2026 Published by Elsevier B.V. on behalf of Chinese Chemical Society and Institute of Materia Medica, Chinese Academy of Medical Sciences.

Cyclic trinuclear complexes are coordination compounds featuring a ring structure with three metal ions bridged by organic ligands [1–3]. While these complexes show promise in chemical sensing, solid-state lighting, full-color displays, and catalysis [4–6], their limited air stability and typical bulk material form hinder their broader application, especially in catalytic processes. Strategies to address these limitations include utilizing CTCs as building blocks in covalent metal-organic frameworks (CMOFs) *via* condensation reactions with organic linkers, which enhances catalytic activity while preserving CTCs integrity [7–9]. For instance, Wei *et al.* have reported the preparation of Cu(I) CMOFs nanosheets, which exhibited enhanced catalytic activity compared to their bulk-phase counterparts [10]. Despite these advancements, a robust method to produce stable, nanostructured CTCs with high dispersibility and catalytic efficiency remains a significant challenge.

Diblock copolymers are polymer chains composed of two distinct blocks, each made up of different monomers that can have varying chemical or physical properties. The two blocks are typically linked by a covalent bond, and their properties, such as solubility, polarity, or crystallinity, can be tuned to create specific functional materials [11–14]. By designing diblock copolymers with specific functional groups, many studies have shown that double hydrophilic diblock copolymers, where both blocks are water-soluble, can act as crystal modifiers [15–18]. The presence of these functional groups can modify the surface properties of crystals, stabilize nanoparticles, or control the size and morphology of the crystalline structures [19–24]. This enables fine-tuning of material properties, such as their optical, electronic, or mechanical characteristics, by controlling the interface between the copolymer and the crystal surface [25–27]. More importantly, the chemical reactivity of one of the blocks in a diblock copolymer can drive the formation of copolymer aggregates, providing a versatile approach for the creation of copolymer nano-objects [28–30]. The ability to manipulate the self-assembly behavior *via* chemical reactions allows for precise control over the morphology and functionality of

* Corresponding authors.
E-mail addresses: jizheng@jnu.edu.cn (J. Zheng), rjwei@jnu.edu.cn (R.-J. Wei), yinning@jnu.edu.cn (Y. Ning).

https://doi.org/10.1016/j.cclet.2025.111535
1001-8417/© 2026 Published by Elsevier B.V. on behalf of Chinese Chemical Society and Institute of Materia Medica, Chinese Academy of Medical Sciences.

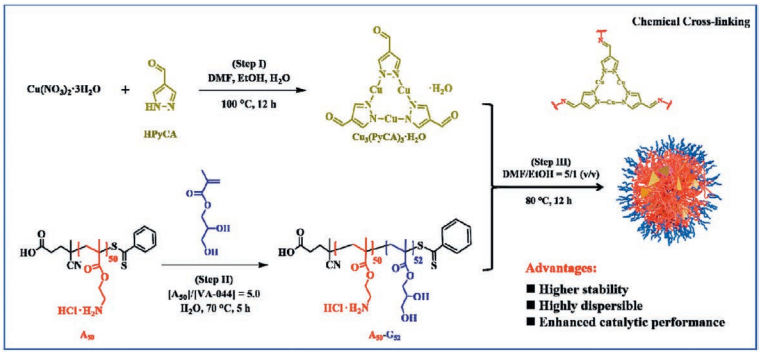


Fig. 1. Schematic illustration of the synthesis of A_{50}-G_{52}-$Cu_3(PyCA)_3$ hybrid nanoparticles. Step I: $Cu_3(PyCA)_3{\cdot}H_2O$ was synthesized *via* a solvothermal reaction between $Cu(NO_3)_2{\cdot}3H_2O$ and HPyCA in a mixture solvent. Step II: A_{50}-G_{52} diblock copolymers were synthesized through RAFT polymerization in aqueous media. Step III: The formation of A_{50}-G_{52}-$Cu_3(PyCA)_3$ hybrid nanoparticles was achieved by chemical cross-linking reaction between the primary amine groups of the A_{50} block and the aldehyde groups of $Cu_3(PyCA)_3{\cdot}H_2O$.

these copolymer structures [31,32]. By leveraging the chemistry of diblock copolymers, this approach has enabled the development of a wide range of nanoscale materials with tailored properties for a variety of technological and industrial uses [33,34].

In the present study, we aim to achieve the particleization of CTCs using diblock copolymers as functional agents. Specifically, we synthesize a reactive diblock copolymer, poly(2-aminoethyl methacrylate hydrochloride)$_{50}$-*block*-poly(glycerol monomethacrylate)$_{52}$, *via* RAFT polymerization (Fig. 1). For simplicity, this diblock copolymer is denoted as A_{50}-G_{52}, where "A" refers to the poly(2-aminoethyl methacrylate hydrochloride) block and "G" refers to the poly(glycerol monomethacrylate) block. The subscripts indicate the respective mean degrees of polymerization (DPs) of each block. We hypothesize that, upon interaction with CTCs, the diblock copolymer will self-assemble into aggregates driven by chemical reaction between the amine groups of the A block and the aldehyde groups present on the CTCs, leading to the formation of colloidally stable hybrid nanoparticles. To confirm the formation and structural characteristics of these nanoparticles, we employed a range of characterization techniques, including transmission electron microscopy (TEM), dynamic light scattering (DLS), Fourier-transform infrared (FT-IR) spectroscopy, and X-ray photoelectron spectroscopy (XPS). These techniques allowed us to investigate the morphology, size distribution, and surface chemical composition of the resulting nanoparticles. Furthermore, the catalytic performance of the hybrid nanoparticles was assessed by evaluating their activity in the Sonogashira cross-coupling reaction, highlighting their potential for applications in catalysis.

The synthetic processes for the preparation of trinuclear copper complexes (tris(μ_2–4-carboxaldehyde-pyrazolato-*N*,*N*')-tri-copper(I) monohydrate, $Cu_3(PyCA)_3{\cdot}H_2O$), diblock copolymers (A_{50}-G_{52}) and hybrid nanoparticles [A_{50}-G_{52}-$Cu_3(PyCA)_3$] were illustrated in Fig. 1. Specifically, $Cu_3(PyCA)_3{\cdot}H_2O$ was prepared following a procedure reported by the Li research group (Step I in Fig. 1) [35]. The detailed synthetic procedure was provided in Supporting information. As a classic trinuclear Cu(I)-based triangular complex, this yellow crystal can be readily and reproducibly achieved by a solvothermal reaction. The crystal structure of the as-prepared $Cu_3(PyCA)_3{\cdot}H_2O$ is consistent with the literature, as determined by powder X-ray diffraction (PXRD) (Fig. S1 in Supporting information). TEM analysis revealed that $Cu_3(PyCA)_3{\cdot}H_2O$ are aggregates with irregular morphologies (Fig. 2a).

RAFT polymerization, a controlled/living radical polymerization technique that allows for precise control over molecular weight, polymer architecture, and polymer composition [36,37], was utilized for the controlled synthesis of A_{50}-G_{52} diblock copolymers. First, poly(2-aminoethyl methacrylate hydrochloride)$_{50}$ macromolecular chain transfer agent (A_{50} macro-CTA) was prepared in a mixed solvent of water/ethanol (50/50, w/w, Fig. S2 in Supporting information); Subsequently, such a macro-CTA was further chain extended with glycerol monomethacrylate monomer, producing poly(2-aminoethyl methacrylate hydrochloride)$_{50}$-*block*-poly(glycerol monomethacrylate)$_{52}$ diblock copolymers (A_{50}-G_{52}, Step II in Fig. 1)). The DP of such diblock copolymers was determined by proton nuclear magnetic resonance spectroscopy (^{1}H NMR). The A_{50} macro-CTA is water-soluble. After chain-extension with poly(glycerol monomethacrylate) block, the resulting A_{50}-G_{52} diblock copolymer can be dissolved in various solvents, including DMF, DMSO and H_2O (Fig. S3 in Supporting information). Gel permeation chromatography analysis showed that both A_{50} macro-CTA and A_{50}-G_{52} diblock copolymer exhibited relatively narrow molecular weight distributions (Fig. S4 in Supporting information), indicating the polymerizations were under good RAFT control [38]. Each block of the A_{50}-G_{52} diblock copolymer possesses an appropriate chain length, which is considered critical for the successful formation of A_{50}-G_{52}-$Cu_3(PyCA)_3$ hybrid nanoparticles. Specifically, the A_{50} block is sufficiently long to enable effective interaction with $Cu_3(PyCA)_3{\cdot}H_2O$, while the G_{52} block serves as a steric stabilizer, imparting good colloidal stability to the resulting hybrid structures.

No significant features were observed by TEM for A_{50}-G_{52} diblock copolymers (Fig. 2b). This observation indicated that no self-assembly of the A_{50}-G_{52} diblock copolymers occurred during the solvent evaporation in the preparation of the TEM sample. However, by mixing $Cu_3(PyCA)_3{\cdot}H_2O$ with the A_{50}-G_{52} diblock copolymers at 80 °C for 12 h (see Step III in Fig. 1), A_{50}-G_{52}-$Cu_3(PyCA)_3$ hybrid nanoparticles were successfully formed, as confirmed by TEM imaging (Fig. 2c). These hybrid nanoparticles exhibited unimodal size distribution, possessing a diameter of approximately 39 nm, as determined by DLS (Fig. 2d). Notably, the diameter determined by DLS was larger than that observed by TEM, which can be attributed to two factors: (1) The A_{50}-G_{52}-$Cu_3(PyCA)_3$ hybrid nanoparticles are in a swollen state in DMF media during the DLS measurement, and it is reasonable to expect that swollen nanoparticles are larger than their dry-state counterparts [39], and (2) DLS measures the hydrodynamic diameter, which includes the stabilizer coronas surrounding the nanoparticles. Both of these factors could contribute to the observed discrepancy [40,41].

The process by which A_{50}-G_{52}-$Cu_3(PyCA)_3$ hybrid nanoparticles form upon interaction between $Cu_3(PyCA)_3{\cdot}H_2O$ and A_{50}-G_{52} diblock copolymers is of considerable interest. Each $Cu_3(PyCA)_3{\cdot}H_2O$ contains three aldehyde groups, while each A_{50}-G_{52} diblock copolymer possesses fifty amine groups. These two types of chemical groups can react to form Schiff bases. From a polymer

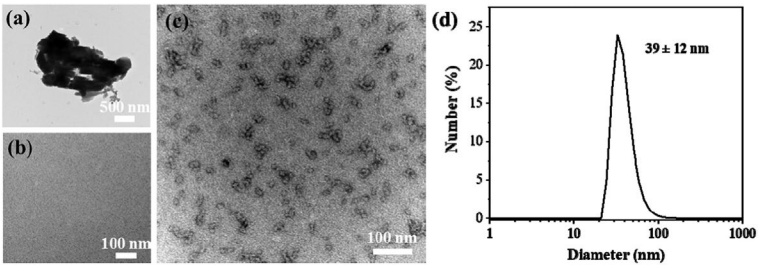


Fig. 2. Representative TEM images of (a) $Cu_3(PyCA)_3{\cdot}H_2O$, (b) A_{50}-G_{52} diblock copolymers; and (c) A_{50}-G_{52}-$Cu_3(PyCA)_3$ hybrid nanoparticles. (d) Hydrodynamic diameter of A_{50}-G_{52}-$Cu_3(PyCA)_3$ hybrid nanoparticles, as determined by DLS.

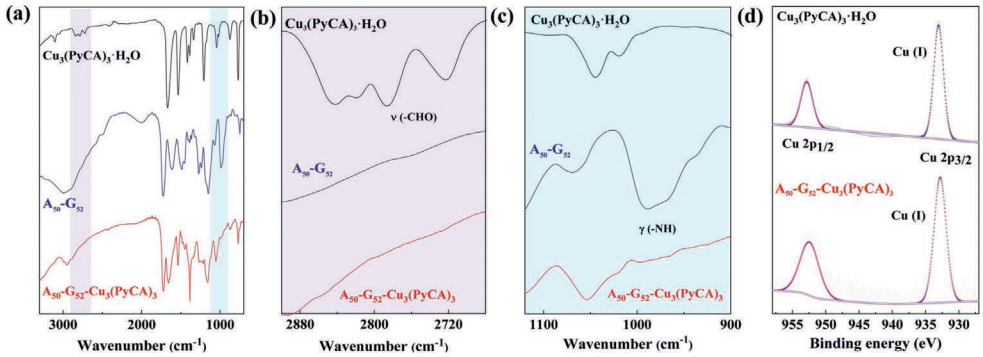


Fig. 3. Characterization of A_{50}-G_{52}-$Cu_3(PyCA)_3$ hybrid nanoparticles. (a) FT-IR spectra of $Cu_3(PyCA)_3{\cdot}H_2O$, A_{50}-G_{52} diblock copolymers, and A_{50}-G_{52}-$Cu_3(PyCA)_3$ hybrid nanoparticles. (b) Enlarged FT-IR spectra showing the disappearance of aldehyde group. (c) Enlarged FT-IR spectra highlighting the disappearance of the out-of-plane bending peak of the amine group. (d) XPS profiles of Cu 2p region of $Cu_3(PyCA)_3{\cdot}H_2O$ and A_{50}-G_{52}-$Cu_3(PyCA)_3$ hybrid nanoparticles.

chemistry perspective, $Cu_3(PyCA)_3$ can function as a cross-linker for the A_{50}-G_{52} diblock copolymers. Indeed, FT-IR spectra showed that an absorption band corresponding to the Schiff base C=N stretching vibration was observed for A_{50}-G_{52}-$Cu_3(PyCA)_3$ hybrid nanoparticles (Fig. 3). Accordingly, the characteristic stretching bands of the aldehyde (2787 and 2723 cm^{-1}) and out-of-plane bending peak of the primary amine were significantly attenuated (Figs. 3b and c). These findings suggested the formation of Schiff base. Unfortunately, after the formation of the hybrid nanoparticles, $Cu_3(PyCA)_3$ lost its crystalline structure since the $Cu_3(PyCA)_3$ species are chemically anchored into the A_{50}-G_{52}-$Cu_3(PyCA)_3$ hybrid nanoparticles. Consequently, it was challenging to analyze $Cu_3(PyCA)_3$ within the hybrid nanoparticles by PXRD. Nevertheless, XPS study indicated the presence of Cu(I) (Fig. 3d), which was further confirmed by Auger peak (Figs. S5a and b in Supporting information). These findings suggested that the $Cu_3(PyCA)_3$ species remain intact during the formation of hybrid nanoparticles.

The formation of A_{50}-G_{52}-$Cu_3(PyCA)_3$ hybrid nanoparticles is most likely driven by the cross-linking reaction between the aldehyde groups of $Cu_3(PyCA)_3{\cdot}H_2O$ and the primary amine groups of the A_{50} block of the A_{50}-G_{52} diblock copolymers. Self-assembly of diblock copolymers can be achieved through various methods, including chemical reactions, pH adjustments, or phase separation [33,42–45]. In the present case, $Cu_3(PyCA)_3{\cdot}H_2O$ acts as a ternary cross-linking agent, facilitating the chemical cross-linking of the A_{50}-G_{52} diblock copolymer. The cross-linked A_{50} blocks then form the core of the A_{50}-G_{52}-$Cu_3(PyCA)_3$ hybrid nanoparticles, with the G_{52} blocks serving as steric stabilizers. This hypothesis is supported by ^1H NMR studies. Comparison of the ^1H NMR spectra of various samples confirmed that the G_{52} block acts as the stabilizer for the hybrid nanoparticles (Fig. 4). This is supported by the fact that only the characteristic peaks of the G_{52} block were observed in the A_{50}-G_{52}-$Cu_3(PyCA)_3$ hybrid nanoparticles. Prior to the completion of hybrid nanoparticle formation, signals from the A_{50} block remain detectable (red arrows in Fig. 4), which confirms

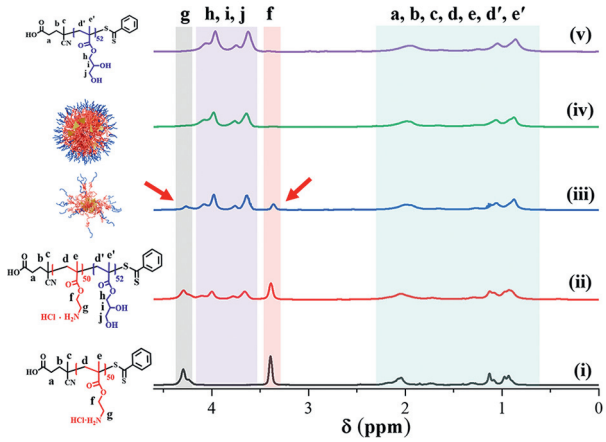
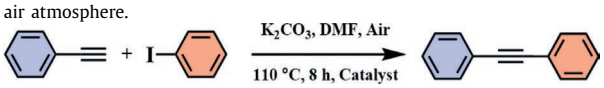


Fig. 4. ^1H NMR characterization confirming the formation of A_{50}-G_{52}-$Cu_3(PyCA)_3$ hybrid nanoparticles that are sterically stabilized by the G_{52} block. ^1H NMR spectra of (i) A_{50} macro-CTA; (ii) A_{50}-G_{52} diblock copolymer; A_{50}-G_{52}-$Cu_3(PyCA)_3$ hybrid nanoparticles synthesized for (iii) 6 and (iv) 12 h, and (v) G_{52} macro-CTA. Red arrows indicate the presence of the pendant -CH_2- groups originating from the A_{50} block of A_{50}-G_{52}; however, their relative intensity compared to A_{50}-G_{52} is significantly reduced. Both of these observations suggest that the formation of A_{50}-G_{52}-$Cu_3(PyCA)_3$ hybrid nanoparticles is underway.

the gradual formation of the A_{50}-G_{52}-$Cu_3(PyCA)_3$ hybrid nanoparticles.

It is well-known that the stability of Cu(I)-based CTCs is relatively low due to their susceptibility to rapid oxidation, which readily converts Cu(I) to Cu(II) ions [3,46–54]. Notably, A_{50}-G_{52}-$Cu_3(PyCA)_3$ hybrid nanoparticles exhibited superior stability compared to the pristine $Cu_3(PyCA)_3{\cdot}H_2O$ species. XPS analysis revealed that copper remained its monovalent state in the A_{50}-G_{52}-Cu_3PyCA_3 hybrid nanoparticles even after storage for over six months (Fig. S6 in Supporting information). In contrast, Cu(II) was

Table 1
Sonogashira cross-coupling reaction in the presence of various catalysts. The reaction conversion was determined by gas chromatography-mass spectrometry (GC-MS) analysis, and each experiment was conducted in triplicate. Reaction conditions: phenylacetylene (0.5 mmol), iodobenzene (1.2 equiv.), K_2CO_3 (30 mg), DMF (4 mL), air atmosphere.



Entry	Catalyst	Conversion (%)
1	None	0
2	A_{50}-G_{52}	0
3	CuCl	0
4	$Cu_3(PyCA)_3{\cdot}H_2O$	~70
5	A_{50}-G_{52}-$Cu_3(PyCA)_3$	>99

observed in the pristine $Cu_3(PyCA)_3{\cdot}H_2O$ species after just one month, as indicated by the appearance of satellite peaks associated with Cu(II) (Fig. S6a). In addition, both TEM study and DLS study indicated the morphology and size of A_{50}-G_{52}-$Cu_3(PyCA)_3$ hybrid nanoparticles remain unchanged (Figs. S6b and c), further confirming their stability. Furthermore, thermogravimetric analysis (TGA) demonstrated that the A_{50}-G_{52}-$Cu_3(PyCA)_3$ hybrid nanoparticles were thermally stable up to 200 °C (Fig. S7 in Supporting information), providing a solid foundation for subsequent thermal catalysis studies.

The Sonogashira cross-coupling reaction, typically used to synthesize alkynylated aromatic compounds, is a widely used organic reaction that forms a carbon-carbon bond between an aryl or vinyl halide (such as a bromide or iodide) and an alkyne (acetylene or substituted alkynes) in the presence of a palladium catalyst and a copper co-catalyst, usually in the presence of a base [55,56]. To explore the catalytic potential of the A_{50}-G_{52}-$Cu_3(PyCA)_3$ hybrid nanoparticles, we conducted a model reaction between phenylacetylene and iodobenzene. As shown in Table 1, the reaction was carried out in DMF solvent with K_2CO_3 as the base. As anticipated, no conversion was observed when A_{50}-G_{52} or CuCl was used in control experiments. In the presence of $Cu_3(PyCA)_3{\cdot}H_2O$, a conversion of approximately 70 % was achieved, confirming that $Cu_3(PyCA)_3{\cdot}H_2O$ is capable of catalyzing the reaction. Remarkably, when A_{50}-G_{52}-$Cu_3(PyCA)_3$ hybrid nanoparticles were used under identical conditions, the conversion increased to >99 %.

Notably, no homo-coupled byproduct, diphenyldiacetylene, which typically forms *via* a Glaser-type coupling reaction in air, was detected in the presence of A_{50}-G_{52}-$Cu_3(PyCA)_3$ hybrid nanoparticles, highlighting the high selectivity of these catalysts. This represents a significant advantage over the Sonogashira cross-coupling reaction catalyzed by conventional copper catalysts (Table S1 in Supporting information) [57,58]. More importantly, these hybrid nanoparticles exhibited excellent stability and recyclability, maintaining their catalytic performance after five catalytic cycles (Fig. 5a). This is because the steric G_{52} block imparts colloidal stability to the A_{50}-G_{52}-$Cu_3(PyCA)_3$ hybrid nanoparticles and is unresponsive to pH variations. Therefore, changes in pH have no significant effect on the colloidal stability of the hybrid nanoparticles. Furthermore, we extended the use of these hybrid nanoparticles to catalyze reactions with various substituted aryl iodides (including methyl, methyl ester, ethyl ester, and amine derivatives), exhibiting high yields in each case (Fig. 5b). The resulting products were characterized by NMR (Figs. S8-S17 in Supporting information). We attribute the enhanced catalytic performance to the chemical anchoring of $Cu_3(PyCA)_3$ within the A_{50}-G_{52}-$Cu_3(PyCA)_3$ hybrid nanoparticles. Under the catalytic conditions described above, the A_{50}-G_{52}-$Cu_3(PyCA)_3$ nanoparticles adopt a swollen state, which facilitates the easy accessibility of reagents to the $Cu_3(PyCA)_3$ species, which located at the swollen core. Additionally, the spatial separation

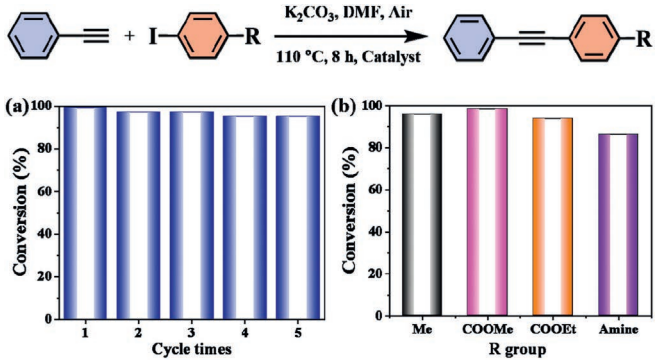


Fig. 5. (a) Recyclability and (b) substrate scope of A_{50}-G_{52}-$Cu_3(PyCA)_3$ catalyzed by hybrid nanoparticles in the Sonogashira cross-coupling reaction.

of each $Cu_3(PyCA)_3$ unit within the nanoparticles allows them to function as a homogeneous catalyst, thereby promoting the rapid progression of the reaction.

In conclusion, we synthesized a unique diblock copolymer, A_{50}-G_{52}, in which the A_{50} block contains reactive amine groups, and the G_{52} block bears *cis*-diol groups, *via* RAFT polymerization. We demonstrate that A_{50}-G_{52}-$Cu_3(PyCA)_3$ hybrid nanoparticles can be readily prepared by the chemical reaction between $Cu_3(PyCA)_3{\cdot}H_2O$ and A_{50}-G_{52} diblock copolymers. Structural characterization using TEM, FT-IR, ^1H NMR, and XPS confirmed that the $Cu_3(PyCA)_3$ species are anchored within the core of the hybrid nanoparticles, while the G_{52} block acts as a steric stabilizer, ensuring high dispersibility in various solvents. Remarkably, these hybrid nanoparticles exhibited enhanced catalytic efficiency and excellent recyclability in the Sonogashira cross-coupling reaction. This work highlights a novel strategy for particleizing CTCs through the rational design of reactive block copolymers, enabling the synthesis of CTC-based functional materials with improved stability and catalytic performance.

CRediT authorship contribution statement

Huahua Cui: Writing – review & editing, Writing – original draft, Investigation. **Baiyao Liu:** Methodology. **Qin Li:** Methodology. **Guo-Quan Huang:** Methodology. **Xu Chen:** Methodology. **Biao Xiong:** Investigation. **Jiahao Zhang:** Methodology. **Ji Zheng:** Writing – review & editing. **Rong-Jia Wei:** Writing – review & editing. **Yin Ning:** Writing – review & editing. **Dan Li:** Writing – review & editing.

Declaration of competing interest

The authors declare that they have no known competing financial interests or personal relationships that could have appeared to influence the work reported in this paper.

Acknowledgments

This study was financially supported by the Fundamental Research Funds for the Central Universities (No. 21621032), and the Basic and Applied Basic Research Project of Guangzhou (No. 202201010237). The Analysis and Testing Center of Jinan University is thanked for TEM support.

Supplementary materials

Supplementary material associated with this article can be found, in the online version, at doi:10.1016/j.cclet.2025.111535.

References

[1] J. Zheng, H. Yang, M. Xie, et al., Chem. Commun. 55 (2019) 7134–7146.
[2] R. Galassi, M.A. Rawashdeh-Omary, H.V.R. Dias, et al., Comments Inorg. Chem. 39 (2019) 287–348.
[3] J. Zheng, Z. Lu, K. Wu, et al., Chem. Rev. 120 (2020) 9675–9742.
[4] A.A. Titov, V.A. Larionov, A.F. Smol'yakov, et al., Chem. Commun. 55 (2019) 290–293.
[5] D. Parasar, T.T. Ponduru, A. Noonikara-Poyil, et al., Dalton Trans. 48 (2019) 15782–15794.
[6] V.A. Larionov, A.R. Stashneva, A.A. Titov, et al., J. Catal. 390 (2020) 37–45.
[7] R.J. Wei, H.G. Zhou, Z.Y. Zhang, et al., CCS Chem. 3 (2021) 2045–2053.
[8] H.G. Zhou, R.Q. Xia, J. Zheng, et al., Chem. Sci. 12 (2021) 6280–6286.
[9] H. Duan, X. Chen, Y.N. Yang, et al., J. Mater. Chem. A 11 (2023) 12777–12783.
[10] R.J. Wei, P.Y. You, H. Duan, et al., J. Am. Chem. Soc. 144 (2022) 17487–17495.
[11] H. Feng, X. Lu, W. Wang, et al., Polymers 9 (2017) 494–524 (Basel).
[12] H.A. Klok, S. Lecommandoux, Adv. Mater. 13 (2001) 1217–1229.
[13] M. Stefik, S. Guldin, S. Vignolini, et al., Chem. Soc. Rev. 44 (2015) 5076–5091.
[14] Y.F. Zhang, K.W. Zeng, H.S. Peng, Sci. China Mater. 68 (2025) 105–109.
[15] J. Hwang, T. Heil, M. Antonietti, et al., J. Am. Chem. Soc. 140 (2018) 2947–2956.
[16] L. Qi, H. Cölfen, M. Antonietti, Angew. Chem. Int. Ed. 39 (2000) 604–607.
[17] H. Li, G. Xue, J. Wu, et al., Chin. Chem. Lett. 28 (2017) 2121–2124.
[18] S. Ayala, K.C. Bentz, S.M. Cohen, Chem. Sci. 10 (2019) 1746–1753.
[19] H. Cölfen, Macromol. Rapid Commun. 22 (2001) 219–252.
[20] L. Qi, H. Cölfen, M. Antonietti, Chem. Mater. 12 (2000) 2392–2403.
[21] D. Zhang, L. Qi, J. Ma, et al., Chem. Mater. 14 (2002) 2450–2457.
[22] Y. Ning, L.A. Fielding, J. Nutter, et al., Angew. Chem. Int. Ed. 58 (2019) 4302–4307.
[23] M. Öner, J. Norwig, W.H. Meyer, et al., Chem. Mater. 10 (1998) 460–463.
[24] X. Sun, Z. Liang, J. Zhang, et al., Chin. Chem. Lett. 36 (2025) 111205.
[25] S.H. Yu, H. Cölfen, J. Hartmann, et al., Adv. Funct. Mater. 12 (2002) 541–545.
[26] D. Zhang, L. Qi, J. Ma, et al., Chem. Mater. 13 (2001) 2753–2755.
[27] Y. Dong, Z. Liu, Y. Ning, et al., Chem. Mater. 34 (2022) 3357–3364.
[28] S. Darling, Prog. Polym. Sci. 32 (2007) 1152–1204.
[29] N.A. Lynd, A.J. Meuler, M.A. Hillmyer, Prog. Polym. Sci. 33 (2008) 875–893.
[30] J. Hou, B. Tu, Q. Zeng, et al., Chin. Chem. Lett. 31 (2020) 353–356.
[31] W. Li, M. Müller, Prog. Polym. Sci. 54 (2016) 47–75.
[32] A. Taubert, A. Napoli, W. Meier, Curr. Opin. Chem. Biol. 8 (2004) 598–603.
[33] J.C. Eloi, D.A. Rider, G. Cambridge, et al., J. Am. Chem. Soc. 133 (2011) 8903–8913.
[34] Y. Lu, J. Lin, L. Wang, et al., Chem. Rev. 120 (2020) 4111–4140.
[35] X. Li, J. Wang, F. Xue, et al., Angew. Chem. Int. Ed. 60 (2021) 2534–2540.
[36] J. Chiefari, Y. Chong, F. Ercole, et al., Macromolecules 31 (1998) 5559–5562.
[37] S. Perrier, Macromolecules 50 (2017) 7433–7447.
[38] S.L. Canning, G.N. Smith, S.P. Armes, Macromolecules 49 (2016) 1985–2001.
[39] Y. Dong, J. Chi, Z. Ren, et al., Angew. Chem. Int. Ed. 62 (2023) e202300031.
[40] Y. Ning, L. Han, M. Douverne, et al., J. Am. Chem. Soc. 141 (2019) 2481–2489.
[41] Y. Ning, Y. Han, L. Han, et al., Angew. Chem. Int. Ed. 59 (2020) 17966–17973.
[42] R.J. Amir, S. Zhong, D.J. Pochan, et al., J. Am. Chem. Soc. 131 (2009) 13949–13951.
[43] R. Deng, M.J. Derry, C.J. Mable, et al., J. Am. Chem. Soc. 139 (2017) 7616–7623.
[44] Y. Mai, A. Eisenberg, Chem. Soc. Rev. 41 (2012) 5969–5985.
[45] H. Yao, Y. Ning, C.P. Jesson, et al., ACS Macro Lett. 6 (2017) 1379–1385.
[46] J.P. Zhang, S. Kitagawa, J. Am. Chem. Soc. 130 (2008) 907–917.
[47] B. Tu, Q. Pang, H. Xu, et al., J. Am. Chem. Soc. 139 (2017) 7998–8007.
[48] G.Q. Huang, X. Chen, J. Zheng, et al., J. Organomet. Chem. 1006 (2024) 122980.
[49] X. Chen, J.Y. Song, J. Zheng, et al., J. Am. Chem. Soc. 146 (2024) 19271–19278.
[50] S. Wang, X. Zhou, X. Ding, et al., ChemSusChem 18 (2025) e202402648.
[51] A. Olbrykh, G. Yakovlev, A. Titov, et al., Crystals 15 (2025) 115.
[52] U.R. Pokharel, F.R. Fronczek, A.W. Maverick, Molecules 30 (2025) 1430.
[53] K. Wu, W. Zhao, L. Huang, et al., J. Am. Chem. Soc. 147 (2025) 13711–13720.
[54] C. Xiong, Q. Li, J. Yang, et al., Chem. Eng. J. 490 (2024) 151881.
[55] A.M. Thomas, A. Sujatha, G. Anilkumar, RSC Adv. 4 (2014) 21688–21698.
[56] T. He, L.L. Wu, X.L. Fu, et al., Chin. Chem. Lett. 22 (2011) 1175–1178.
[57] S.M. Guo, C.L. Deng, J.H. Li, Chin. Chem. Lett. 18 (2007) 13–16.
[58] K.V. Arundhathi, P. Vaishnavi, T. Aneeja, et al., RSC Adv. 13 (2023) 4823–4834.